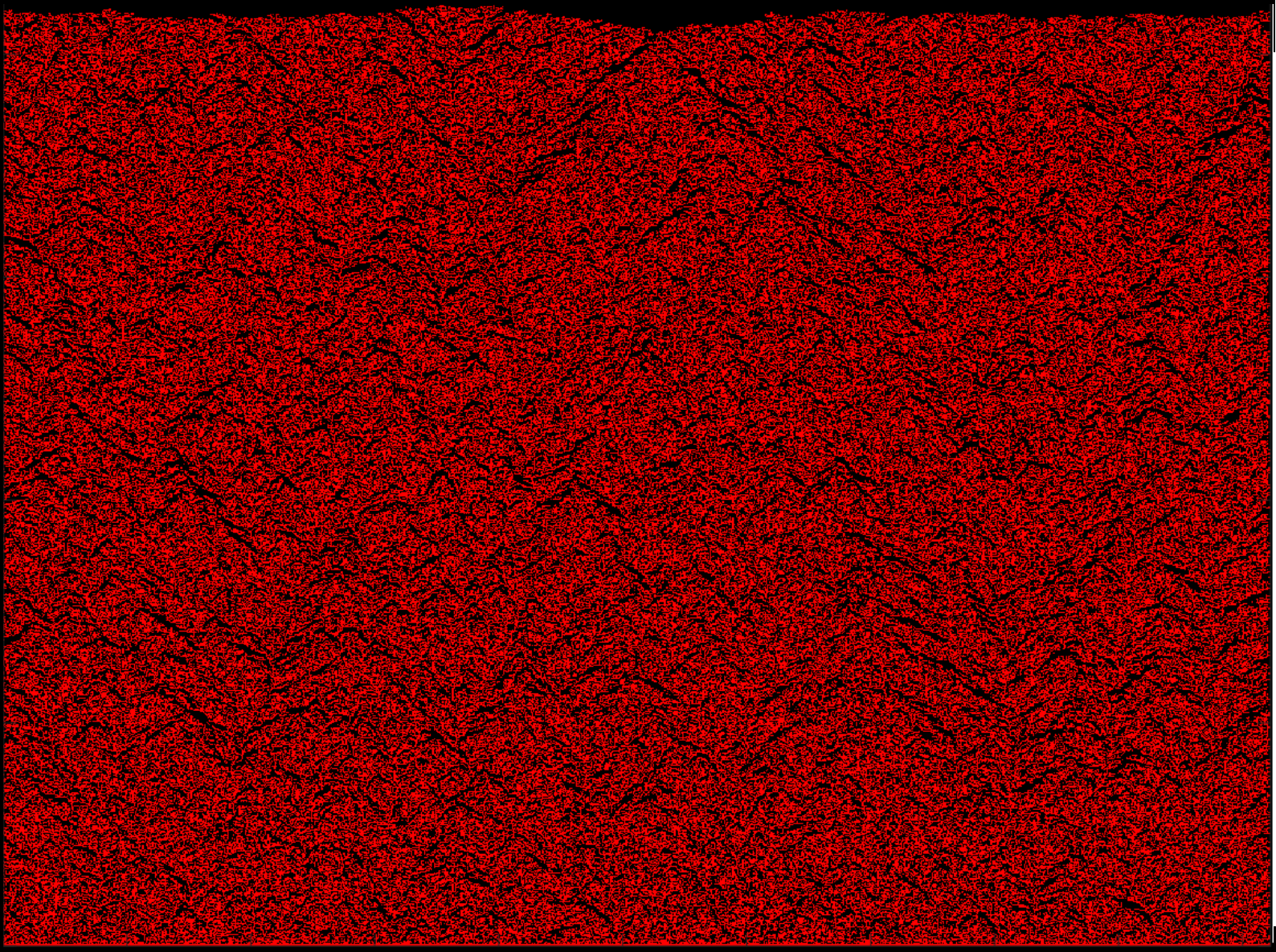

Ballistic Deposition

Oliver Gordon - 4224942 University of Nottingham Scientific Computing

ABSTRACT

Ballistic deposition serves as a simple method to explore how the macrostructures of growing aggregates will evolve in ordered, well-defined ways over long periods of time, despite variation in the rules of growth. This is due to underlying KPZ (Kardar–Parisi–Zhang) universality classes. Three of the universality classes, α, v and γ were investigated for multiple growth rules, including probability based sticking and height difference based sticking.

When run with a simple simulation there was agreement with the expected values of $\alpha = 0.5, v = \frac{1}{3}$ and $\gamma = 1.5$, with $\alpha = 0.4725 \pm 0.0399$, $v = 0.3244 \pm 0.0005$ and $\gamma = 1.4565 \pm 0.0845$. Similar results were found for the case of probability based sticking, but it was not possible to investigate height related sticking due to the model used. Deposition at an angle was performed to investigate the empirical tangent rule, which the simulation did not agree with. The evolution of density was also investigated, with density tending to 0.5 for the simple model, and 1 for the probability based model.

INTRODUCTION

The process of random ballistic deposition serves as a simple way to model and study the surface geometry of 2D and 3D bodies[1]. Ballistic deposition is a flux limited process as opposed to being a reaction limited one, as growth is limited by the number of particles available rather than the rules of growth[1]. It is of widespread interest both inside and outside of Physics, with applications ranging from modelling the propagation of flame fronts[2] to the understanding of fractal surfaces[3]. Perhaps the most significant uses, however, regard the formation of thin films[4], directed polymers[2], and various other microstructures[4]. This is due to inbuilt universality classes[5] causing aspects such as saturation height, microstructure and angle of growth to be highly predictable, despite the random nature of depositing particles[4].

Investigations regarding ballistic deposition were initially performed by Vold in 1963[5], and later Sutherland in 1966[6] in order to improve their understanding of colloidal aggregation[5]. Although they were not successful, they laid the framework for future development of colloidal aggregation models[7]. The universality classes were largely developed by Karder, Parisi and Zhang in 1986[8]. In their models, particles fall linearly (and hence in a ballistic fashion), with the model considered to be 'on lattice' as deposited particles are confined to a grid[1].

To demonstrate the universality laws, the lattice must first be saturated. This occurs when particles correlate along the width, l, of the area being deposited on. Lattices of width l = 8 can require approximately $N \approx$ 10,000 drops, whilst large lattices of l = 1024 can require $N \approx$ 1,000,000 drops[9] in order to saturate the lattice. Vold and Sutherland's calculations, however, involved at most N = 160 particles[5].

To form a simple aggregate, a random position along the width of the lattice is selected for a particle to drop from. This particle will then stick to the block that is immediately to the right or left or below it (depending on which of those blocks is the highest). The $N_{i=2}{}^{th}$ particle is then dropped, then the $N_{i=3}{}^{rd}$ and so on. By repeating this process for N number of depositions, complex structures can be formed. Permutations for the first three drops, $i = 1,2,3$, are shown in Figure 1. The grid positions that the next block could stick to are referred to as active sites and are at heights, h, The active sites for all of the $N_{i=2}$ drop permutations are shown in Figure 2.

These methods can be extended to the third dimension, with varying probability of sticking, different sized blocks, angular dropping, and maximum height difference between side stuck blocks and the blocks surrounding them. However, the universality classes should remain constant in each of these scenarios[4]. As a result, computer models can predict how the macrostructure of much larger, real surfaces will evolve over long timescales even when the microstructure of the aggregate changes.

In this project, the universality classes, α, v and γ were investigated for a variety of sticking rules, including sticking probability, and height differences. The empirical tangent rule was investigated by depositing particles at angles, and the variation of density with lattice width and sticking probability were also investigated.

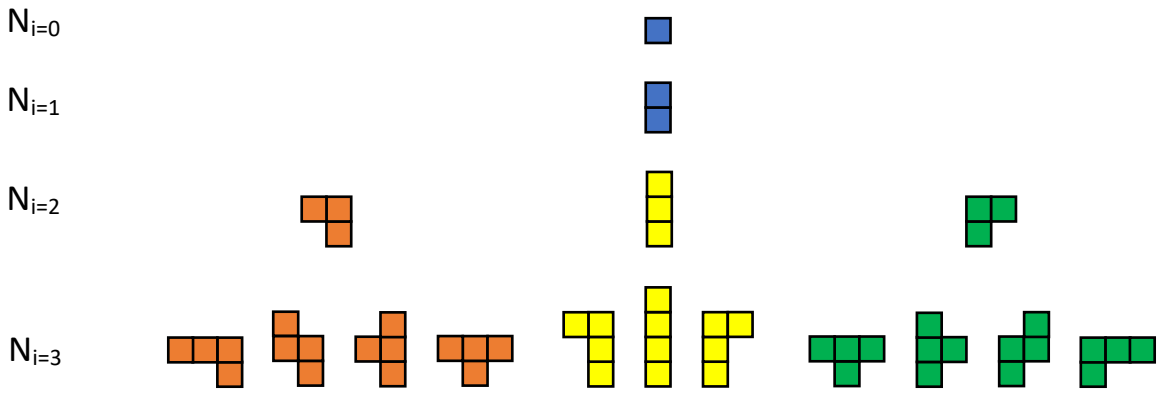

Figure 1: Figure to demonstrate how different structures can be produced during random ballistic deposition. Starting from a base at $N_{i=0}$, a block ($N_{i=1}$) is dropped, and will stick above or to the immediate right or left of it depending on which will be tallest. From there, another block is dropped ($N_{i=2}$), and can stick above or to the right or left of the ($N_{i=1}$) block. This is then repeated again, and over time will form porous but highly ordered structures. Due to the shapes of these combined blocks, they will spread outwards as they grow, resulting in tree shaped microstructures.

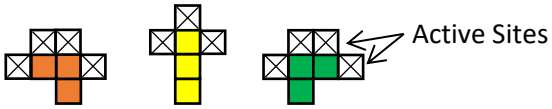

Figure 2: Figure to demonstrate active sites in the ballistic deposition model. The active sites are shown as crossed boxes, and represent the grid sites where the next block to be deposited could stick to. In this case, active sites for the $N_{i=2}$ deposition are shown.

THEORY/METHODS

Three of the universality classes are those of the 'roughness' exponent, α, the 'growth' exponent, v, and the 'crossover' exponent, γ[4]. They have been theorised to have values of $\alpha = 0.5$[8] and $v = \frac{1}{3}$[8] with γ defined as[8]

$$\gamma = \frac{\alpha}{v}. \qquad [1]$$

It is related to α by the equation[10]

$$\gamma + \alpha = 2, \qquad [2]$$

which results in $\gamma = 1.5$. These constants are related to the width of the lattice being deposited on, l, and mean active height, $\bar{h}$, by the equation[11]

$$\xi = l^{\alpha} f(x). \qquad [3]$$

Here, $f(x)$ is a scaling function of particles deposited, $x = \frac{\bar{h}}{l^{\gamma}}$, which converges to $f(x) \sim const.$ for long timescales and $f(x) \sim \bar{h}^{v}$ for short timescales. ξ is defined as the width of the active zone, and is given by the equation,

$$\xi^2 = \frac{1}{l} \sum_{i}^{l} \left(h_j - \bar{h}\right)^2, \qquad [4]$$

where h_j is the active height of each column along l, and j the column number.

During the initial dropping of particles, each column in the lattice is essentially independent and will grow linearly with $N = \bar{h}^{0.5}$, as horizontal sticking is yet to occur. As more particles are dropped, the probability of sticking horizontally increases, and correlations begin to appear across the lattice, with $v = \frac{1}{3}$. At late times, correlations begin to appear across the full width of the lattice, ξ becomes asymptotic, and the lattice is said to be saturated[12]. As a result, the lattice should saturate quicker for smaller values of l. These three stages are demonstrated in Figure 3.

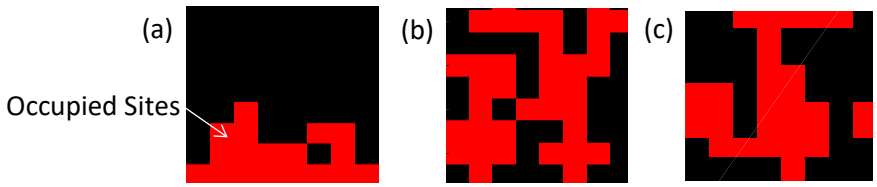

Figure 3: Figure to demonstrate how correlations appear over time in the ballistic deposition model, as shown on an $l = 8$ wide lattice. At early times (section a), each particle on the lattice is effectively independent of one another, and growth is rapid. At intermediate times (section b), horizontal links begin to partially appear along the width of the lattice, producing correlation. At late times (section c), the full width of the lattice is fully correlated and remains so forever. At this point, the lattice is said to be saturated. This process is governed by KPZ (Kardar–Parisi–Zhang) universality classes.

When the program is run, an empty lattice matrix of fixed width, $l + 2$, is formed (with the first and last columns used for periodic wrapping). A flat base is formed by assigning the value 1 to the base of the matrix. A particle is dropped from a position randomly distributed along l. Each dropped particle is compared to the particles below and to the immediate right or left of it, and the highest available particle stuck to. Each grid point occupied by a particle is given the value 1 in the matrix. Periodic wrapping is implemented when a particle is dropped on either the second or second to last column. This is achieved by swapping the first and second to last columns, and the last and second columns. Over time, the lattice increases in height in segments to accommodate more particles.

After each N_i^{th} particle is dropped, each grid point on the lattice that is an active site is assigned the value 2. Each column neighbouring the dropping position has active height, h_j, calculated and then stored to a pre-allocated matrix contaniing all values of h_j along l. After N particles have been dropped, the N_i^{th} values of h_j are combined and $\overline{h}$ calculated. Using Equation 4, ξ is then calculated for each particle dropped, and the results stored to file. Raw results are also saved for $\overline{h}$, average block height, and density.

The lattice matrix is then reset, and deposition repeated multiple times. After these repeats, the program itself is then repeated for a variety of lattice widths. After this, all repeats for all l are averaged, and stored to file. The value that ξ converges to, ξ_0, is calculated through a linear regression curve fit on the asymptotic part of a graph of ξ vs $\bar{h}$, and stored with its error.

v is calculated with the function $\xi \sim \bar{h}^v$ by curve fitting a graph of $\ln(\xi_0)$ vs $\ln(\bar{h})$ at intermediate timescales $(\bar{h} \ll l)$. A graph of $ln(\xi_0)$ vs $ln(l)$ is then plotted, which as of Equation 3 will have a gradient of α. γ can then be found with Equation 1 or 2. A flow diagram for the dropping program is shown in Figure 4.

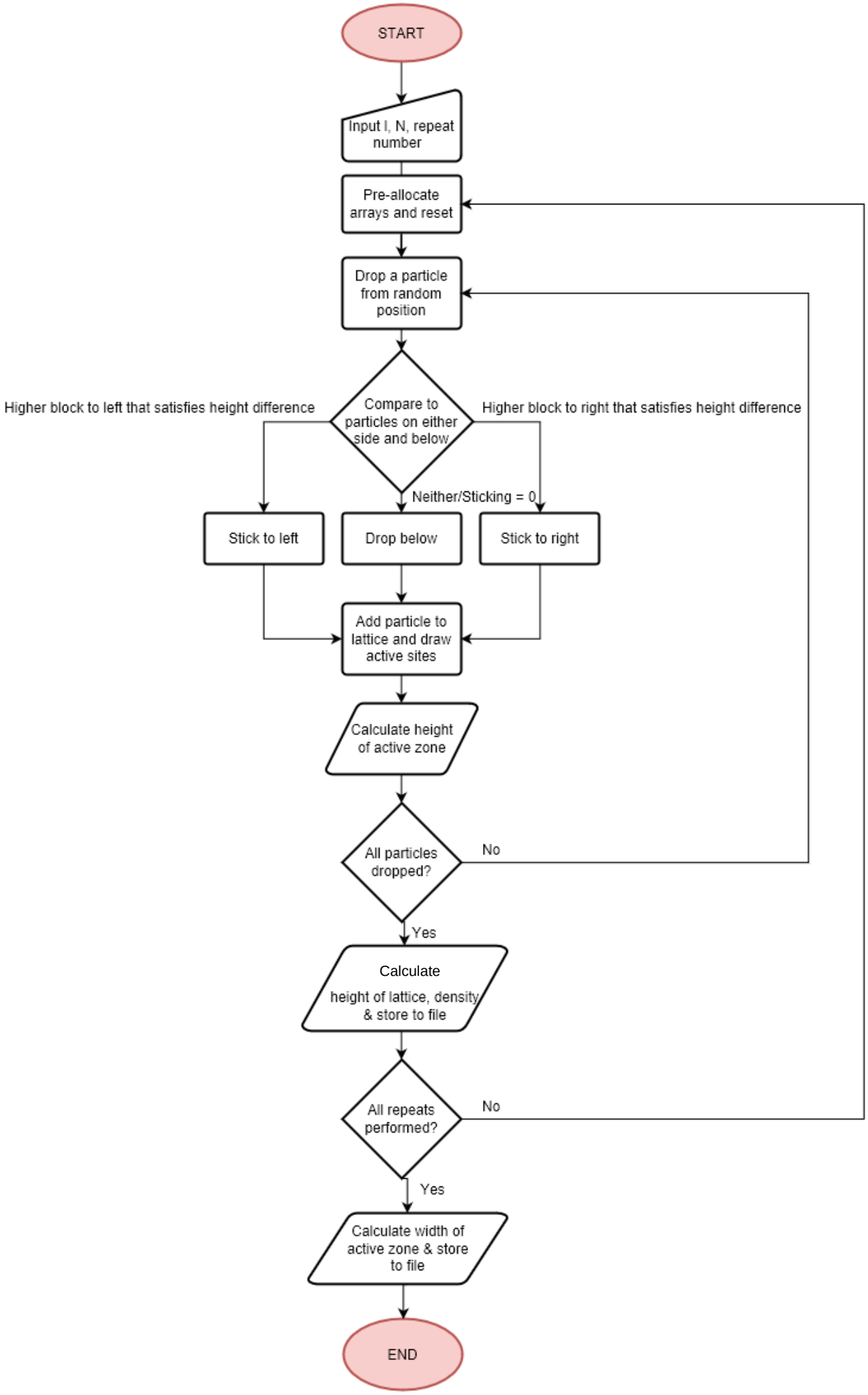

Figure 4: Figure to explain the algorithm used in the ballistic deposition model to deposit particles and calculate various quantities of interest.

In order to effectively demonstrate the universality classes, N must be large enough to saturate the lattice, with more particles required to generate correlations of increasing length l. Significantly more repeats are required at lower values of l, as small variations in h have a greater effect on $\bar{h}$ and thus on ξ as of Equation 4. This is demonstrated in Figure 5. As a result, there is a trade-off to be made between using larger l but requiring larger N, and using smaller l but requiring more repeats. Both situations require more computational time.

More complex sticking rules have also been implemented, such as with sticking probability. First, a fractional probability is input during the initial setup of the program. A vector of N uniformly distributed values between 0 and 1 is generated and then compared with the sticking probability. If the random value is higher, sticking takes on the value 1. If it does not, sticking is instead 0. The N_i^{th} value of this vector is then read out; if it equals 1, the dropping particle sticks. If it equals 0, sticking does not occur and the particle falls down. This is demonstrated in Figure 6.

Another alternative sticking rule implemented is that of height difference. With this rule enabled, particles stuck to the right or left cannot be more than a user specified height difference away from the particle below. This is demonstrated in Figure 7.

The final deposition rule involves deposition at an angle. With this, the base of the lattice is no longer flat, but instead dependant on an input incident angle, θ_i. The base height of each lattice column, b_j, is given by the equation

$$b_j = l_j \tan(\theta_i)\,, \qquad [5]$$

where l_j was the j^{th} column along l. Ballistic deposition then continues as before, but with a vertical offset to the wrapping of $\pm\, b_{j=l}$ on the left and right sides of the lattice respectively. The angle of growth, θ_g, is related to θ_i by the empirical tangent rule equation[13]

$$\tan(\theta_j) = \frac{1}{2}\tan(\theta_i) \qquad [6]$$

Finally density, ρ, can be calculated with the equation[1]

$$\rho = \frac{N}{h_{max} l}, \qquad [7]$$

where h_{max} is the height of the highest particle.

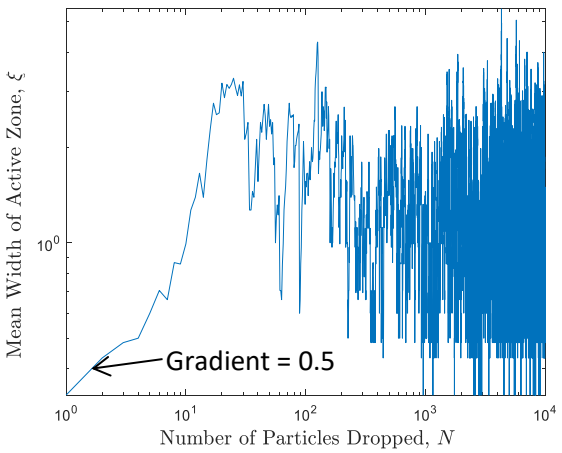

Figure 5: Figure to demonstrate the large amount of noise produced during individual runs of the program, particularly for runs involving short lattice widths (l = 8 is figured here). This was reduced by averaging over a large number of repeats, with 10,000 repeats in this case. Note the smooth initial growth when each column is uncorrelated.

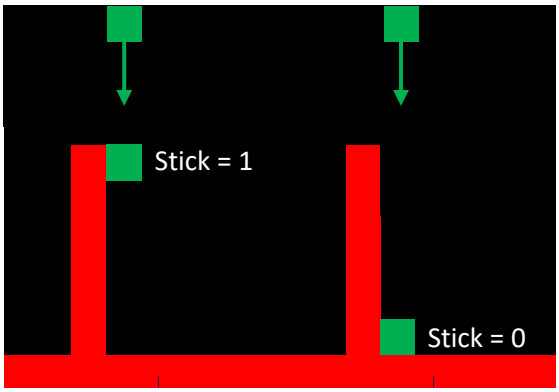

Figure 6: Figure to demonstrate the probability based sticking model. The random number 0 or 1 is generated, whose probability of equalling 1 equates to an input sticking probability. If the number is equal to 1, sticking occurs (as represented on the left). If the number is equal to 0, then the particle drops to the bottom (as seen on the right).

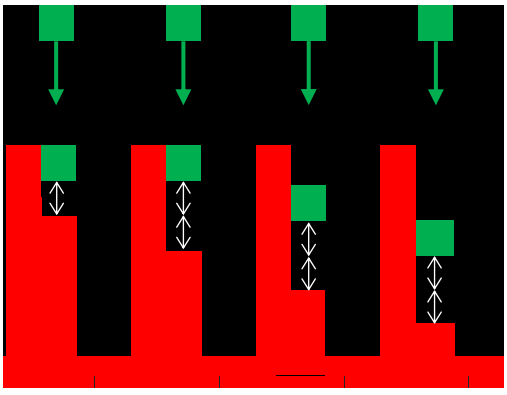

Figure 7: Figure to demonstrate the height difference based sticking model. In the case pictured, a height difference of 2 has been applied, meaning that blocks can only horizontally stick if the block below the sticking position is at most 2 grid points lower.

To verify its accuracy, the program was run with simple sticking rules for values of l between 8 and 256, N between 10,000 and 200,000, and repeats between 10,000 and 1000. The l=256 lattice was used to find $v = 0.3244 \pm 0.0005$, as it had the largest range over which to curve fit. It was then found that $\alpha = 0.4725 \pm 0.0399$, with Equation 1 that $\gamma = 1.4565 \pm 0.0845$ and with Equation 2 that $\gamma + \alpha = 1.929 \pm 0.093$ using error propagation. These values were in good agreement with Equation 2 ($\gamma + \alpha = 2$) and the expected values of α = 0.5, $v = \frac{1}{3}$ and $\gamma = 1.5$ [8]. The results are demonstrated in Figure 8. Due to random noise and the fact that ξ only becomes fully asymptotic at infinite time, obtaining a slightly lower value of α was expected[4], with independent simulations typically finding α between 0.42[7] and 0.48[14], depending on repeat number. More repeats and greater N would have reduced this discrepancy by reducing noise and increasing the timescale.

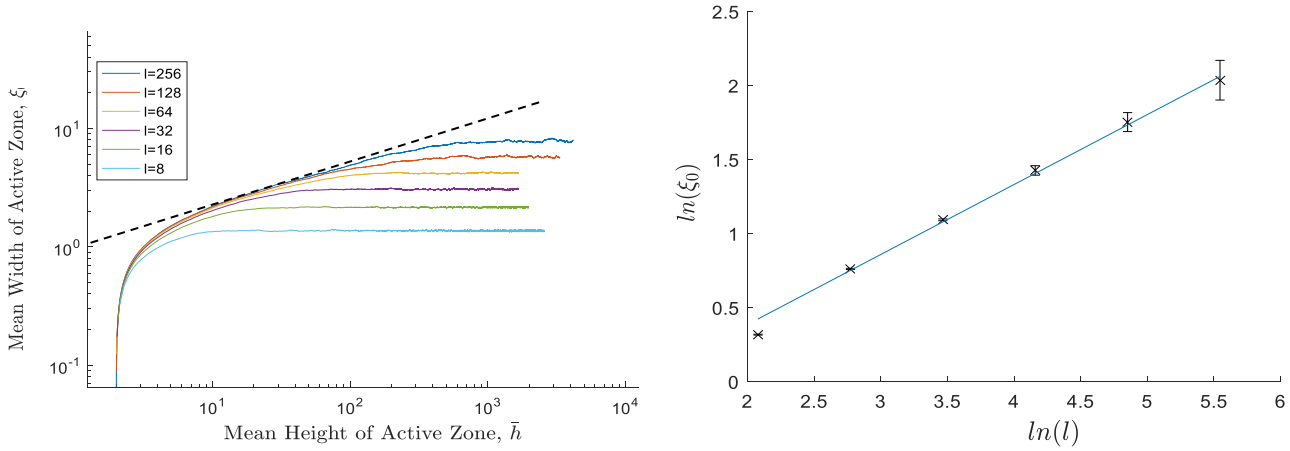

Figure 8: Figure to verify the accuracy of the program developed. When run with simple sticking rules, a graph of $ln(\xi_0)$ vs $ln(l)$ (shown right) gave a gradient of $\alpha = 0.4725 \pm 0.0399$ when fitted with a linear regression fit. The dotted line on a graph of ξ_0 vs $\bar{h}$ (shown left) shows the line fitted to the function $\xi \sim \bar{h}^v$ for the l=256 lattice in order to calculate v, which resulted in $v = 0.3244 \pm 0.0005$. This was very close to the expected value of 0.5 and 1/3 respectively. Lower values of l saturated and become asymptotic sooner, and early time behaviour was irrespective of lattice width.

EXTENDING THE MODEL

Once the program was verified to be accurate, it was modified to have a variable probability of sticking, as explained previously in Figure 6. The program was run for lattices of width l = 8, 16, 32, 64 and 128, with N and the number of repeats kept as before. In each case, this was repeated with sticking probabilities of 20%, 40%, 60%, 80% and 100%. When compared with the simple sticking rules used previously, it was found that sticking probability has little effect (if at all) on the values of v, or on the shape of the evolution of ξ_0 with respect to $\bar{h}$. This is as the universality classes that growth depends on do not change.

It can be seen on Figure 9 that lower sticking probabilities required a greater value of $\bar{h}$ (and therefore N) before saturation occurred. This was as there was a lower probability for horizontal sticking to occur, which decreased the probability of increasing correlation.

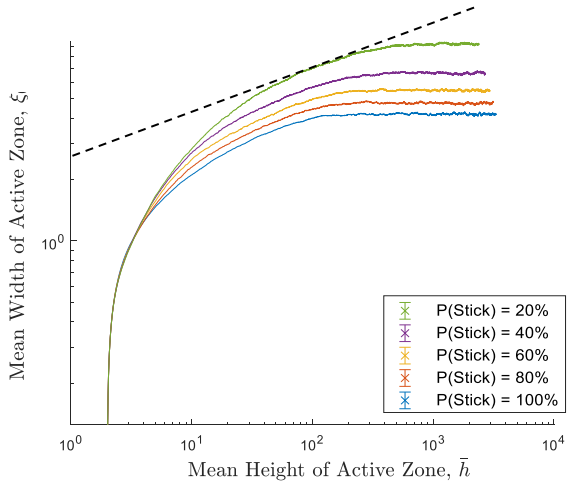

Figure 9: Figure to demonstrate the consistent evolution of ballistic deposition despite the implementation of probability related sticking rules which changed the microstructure formed. Here, different probabilities of sticking were calculated on a l= 64 wide lattice. Higher probabilities of sticking saturated sooner and at lower heights. The black dotted line indicates the fit to which v was determined for 20% probability, $v = 0.3206 \pm 0.0012$.

When curve fitted over a similar range of active heights, v remained near constant for all probabilities, and varied between 0.3206 ± 0.0012 for the highest sticking probability and 0.3054 ± 0.0098 for the lowest. The lowest sticking probability had the longest intermediate time, so was most ideal for calculating v. For the three highest sticking probabilities, there was little effect on α, with α randomly varying from 0.4597 ± 0.0481 to 0.4792 ± 0.0462. This is shown in Figure 10. Here, the range of α was likely due to random noise, as the results were within error bounds. However, α decreased for decreasing probability with $\alpha = 0.3985 \pm 0.0514$ for the 20% probability. This may be because the model made unstuck particles fall down, instead of more realistically slide down. Lower probabilities would have amplified this effect. The sliding model has been shown elsewhere to yield expected values [15].

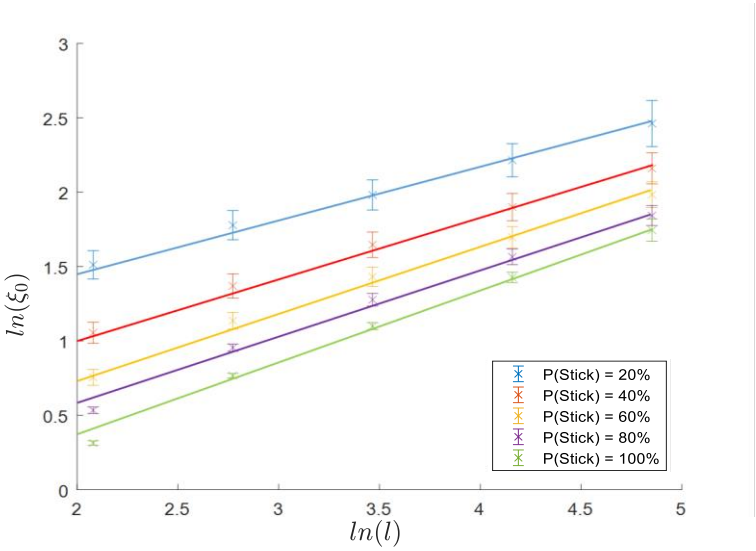

Figure 10: Figure to demonstrate how α, remained close to its expected value of 0.5 despite variation in the probability of sticking. Each colour line represents a different probability of sticking, with the points representing the active height that the system showed asymptotic behaviour at, $\xi_{0,}$ as a function of lattice width, l. It was found (in descending order), $\alpha = 0.3985 \pm 0.0514$, $\alpha = 0.3985 \pm 0.0514$, $\alpha = 0.4597 \pm 0.0481$, $\alpha = 0.4499 \pm 0.0476$, $\alpha = 0.4792 \pm 0.0462$. Although the top two results were significantly lower than the expected value of 0.5, this may be due to a limitation of the model used.

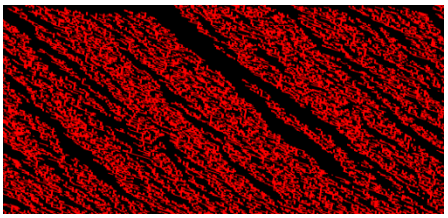

Figure 11: Figure to demonstrate ballistic deposition at an incident angle of 45˚ to the lattice.

Next, the tangent rule was investigated. Particles were fired at incident angles of $\theta_i = 20°, 30°, 40°$ and $50°$ onto lattices of width l = 128,256,512. One example deposition is shown in Figure 11. The average angle of growth, θ_g, was found with a protractor for the four largest 'tears' in the deposition. The error ranges were defined as the range of values measured. As of Equation 6, a graph of $\tan(\theta_j)$ vs $\tan(\theta_i)$ should have a gradient of roughly 0.5 as found with linear curve fitting, and shown in Figure 12. However, the closest gradient found was 0.39±0.03.

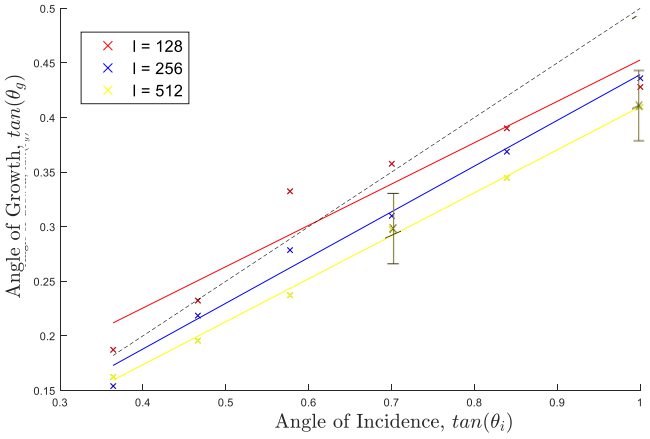

Figure 12: Figure to demonstrate the tangent rule. The tangent rule (shown in dotted black) is theorised to result in a gradient of 0.5, but it was instead found to be 0.35 at best. The tangent rule was found in a physical lab, which may explain the discrepancy.

This result is not surprising, as other simulations have found the tangent rule to not hold particularly well[4]. This is possibly as the rule was developed for a physical deposition, which may have been influenced by its surroundings. There is evidently a correlation between θ_g and θ_i, as the gradient of each line of Figure 12 is roughly similar, despite significant errors (not shown for clarity). Determining θ_g was also problematic for lower θ_i, as smaller 'tears' made the angle of growth less well defined, and few repeats were taken.

Minimum height related sticking, as explained in Figure 7, was then investigated. As shown in Figure 13, it was not possible to obtain a value of α. This is as the lattice never remained (or sometimes never even became) saturated, but often 'uncorrelated' at a random time. Due to the random deposition, some columns would temporarily increase in height slightly faster than their neighbours, leaving a neighbour too low to stick horizontally. Because horizontal sticking results in faster growth, these columns could never stick horizontally again, and were 'left behind'. As shown in Figure 14, this uncorrelated the lattice. A better model would have involved instead checking height difference to the neighbours, but this was not attempted due to time constraints.

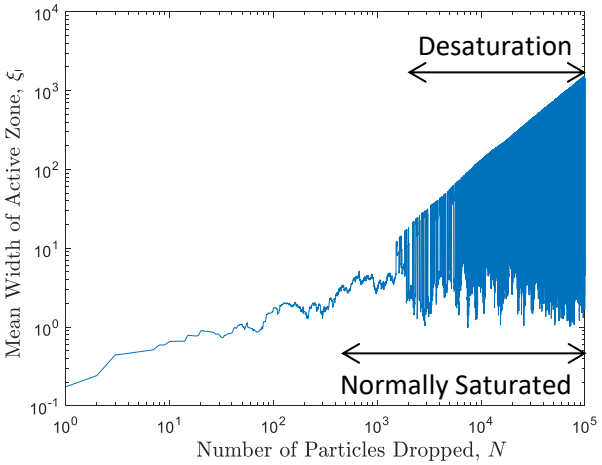

Figure 13: Figure to demonstrate 'desaturation,' for the height based sticking model, which resulted in α not being able to be found. It was found that larger lattices were more likely to de-correlate before reaching the saturation point, while smaller ones were more likely to de-correlate after reaching the saturation point.

By counting the number of times desaturation occurred for various height differences over 50 repeats for lattices of l = 32, 64, 128 with N = 100,000, higher height differences were found to be less likely to desaturate. This is shown in Figure 15. Errors of ± 1 counts had been counted for cases where desaturation is unclear.

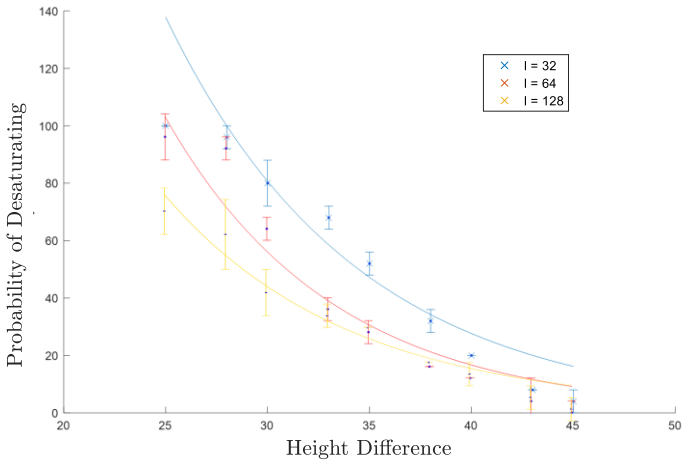

Figure 15: Figure to demonstrate probability of desaturation as a function of height difference. This desaturation meant that the universality classes could not be well demonstrated. A better height based sticking model would require imposing a height restriction on neighbouring particles, but this was not done due to time constraints. It would be expected that α would remain the same.

Density was also investigated. Using data from the simple model, ρ was calculated using Equation 7 and plotted as a function of $\overline{h}$ for multiple values of l. This is shown in Figure 16. At early times, l appeared to have no effect on ρ, which made sense as the particles were not sticking horizontally. When saturated at late times, ρ would tend towards 0.5 blocks per unit area, with lower values of l closer. It was also found that random noise had a miniscule effect on this behaviour; larger lattices with less repeats had small, similar errors to those of smaller lattices. l = 8 tended to 0.4896 ± 0.0001, while l = 256 tended to 0.4665 ± 0.0002.

Density was also investigated for probability based sticking. This is shown in Figure 17. Again, the densities grew identically at early times, before becoming asymptotic when saturated. However, ρ did not tend to 0.5, instead tending higher as sticking probability decreased. This was logical, as lower probabilities of sticking would decrease the average height difference between blocks, thus increasing density. Sticking probabilities of 0% would tend towards a density of 1 block per unit area as no horizontal sticking would occur to leave gaps, so sticking probabilities of increasingly less than 100% would tend towards densities of increasingly less than 1. It was also found that the saturated values of density were almost completely independent of l. The 20% probability saturated at ρ = 0.6476 ± 0.0002 for the l = 64 lattice shown in Figure 17, whilst it saturated at ρ = 0.6321 ± 0.0004 for the l = 8 lattice. This was expected, as the macrostructure should evolve consistently.

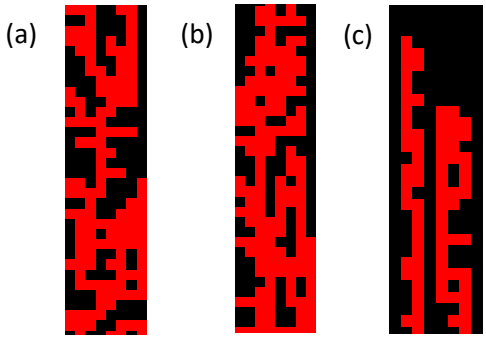

Figure 14: Figure to demonstrate desaturation of the lattice with the height based probability model for the l=8 wide lattice. At some random time (section a), random fluctuations in height would cause one column to get 'left behind,' as it was too low to stick horizontally and gain more than 1 block in height at a time. The lattice could then never be fully correlated. Growth then continued as before (section b), with increasing numbers of columns being left behind, before only thin towers remained (section c).

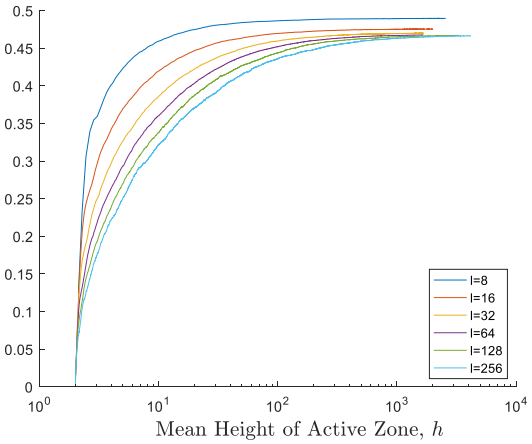

Figure 16: Figure to demonstrate the evolution of density with active zone height for different lattice widths. At early times, the evolution for different l was highly similar, with lines overlapping for the first few hundred depositions. At intermediate times, the densities diverged, but followed the same shape. At later times when the lattice was saturated, density became asymptotic. l = 8 tended to 0.4896 ± 0.0001, with l = 256 lower at 0.4665 ± 0.0002.

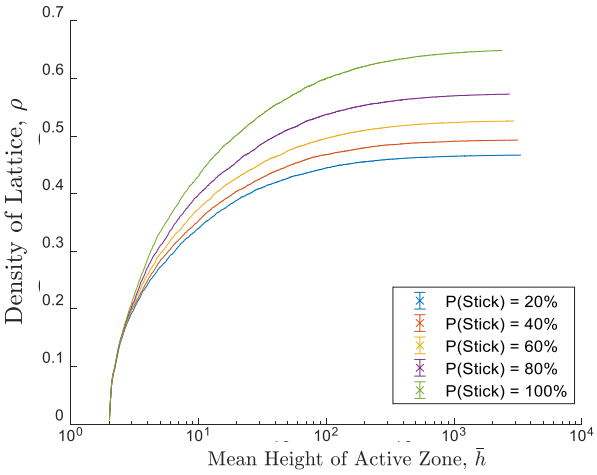

Figure 17: Figure to demonstrate the evolution of density with active zone height for a ballistic deposition model with probability based sticking rules for the l = 64 wide lattice. At early times, densities of various probabilities overlapped. At intermediate times, they followed the same shape, but began to diverge. Lower probabilities had higher densities at saturation, with P(Stick)=20% saturating at ρ = 0.6476 ± 0.0002, and P(Stick) = 100% saturating at ρ = 0.4681 ± 0.0001. These trends remained, regardless of lattice width.

DISCUSSION & CONCLUSION

The KPZ universality classes, a, v and γ mean that the macrostructure of a ballistic deposition will always evolve in the same fashion, regardless of physical setup. When used as scaling factors, as shown in Figure 18, the high dependence of growth on these classes becomes clear. One novel application involves thin film formation, in which it is possible to use evenly spaced single particles (instead of a harder to produce flat base) to form cones, and in doing so for a period of time form flat atomic scaffolds for a variety of scientific uses. This is shown in Figure 19. Other novel applications involve chemically varying probability to manufacture denser films, such as those required by thin film solar panels[16].

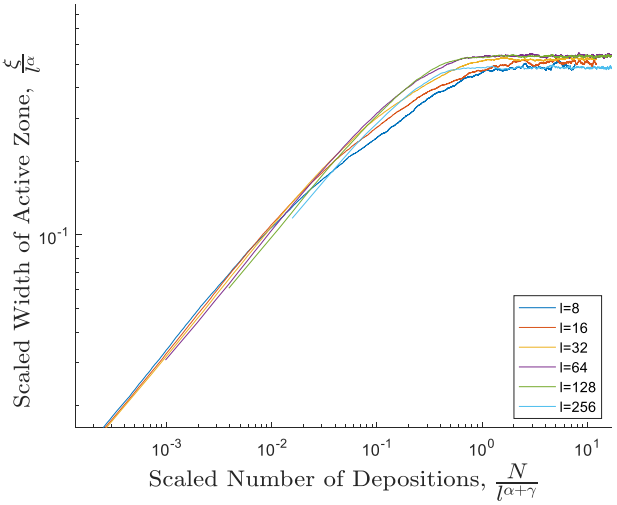

Figure 18: Figure to demonstrate the dependence of macrostructure on universality classes. Once scaled with values found with the program, evolution is a near constant for a variety of structures. (x axis should be t/l^{γ})

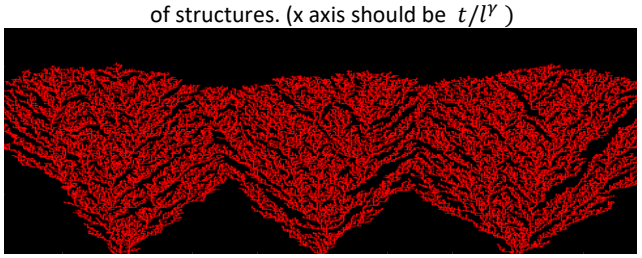

Figure 19: Figure to demonstrate how KPZ universality classes could be exploited to form an atomic scaffold. The universality classes mean that the angle of growth from single points a fixed distance apart will be constant. This can be combined with simple trigonometry to quickly form a nearly flat structure that could be used as an atomic scaffold to perform another experiment on.

The program served as a decent way to demonstrate the universality classes. Even when changing the rules of deposition, a was found to be approximately 0.5, v approximately $\frac{1}{3}$ and γ approximately 1.5. Although a tended away from its expected value for low sticking probabilities, this was likely a limitation of the model used, and implementing a sliding based model would improve upon this. The height based model could not be used to find a due to desaturation, so the height difference to neighbouring particles instead of the height difference to the block below should have been limited. The angle based model would have benefited from an algorithmic filling method to calculate growth angle, which would have allowed for significantly more repeats and lower error ranges when investigating the tangent rule.

There were also difficulties with defining intermediate time-steps along which to calculate v. This had to be determined by hand and was therefore somewhat arbitrary, introducing greater errors to the value found by curve fitting. To reduce this error, the largest range of points that was still visibly straight was used to curve fit. In future, it could be observed that in the same way as $\bar{h} \sim l^{\alpha}$, time, $t \sim l^{\gamma}$. γ could therefore be calculated in a similar way to α, and Equation 2 could then be used to more accurately calculate v.

Improvements could also be made to the program itself. The algorithm used was not particularly efficient, with the functions to find maxima particularly slow. A more efficient algorithm would have involved testing against the 2D vector of active heights to grow the lattice, instead of calculating heights and active heights and forming a matrix for both. This would also eliminate both maximum finding functions. As a result of this inefficiency, depositions and calculations were performed at a rate of approximately 80,000 deposits per second when run on a typical quad core computer. This prevented large lattices requiring upwards of one million particles from being calculated in a reasonable timeframe. As a compromise, multiple computers were used to run extra repeats on smaller lattices more suited to the program developed.

The program could also be extended to further demonstrate the universality investigated. For example, the deposition could be extended to 3D by running the same algorithm along another axis. Alternatively, particles of varying size could be deposited as opposed to the 1D blocks used in this experiment, or multiple blocks could have been allowed to stick at once. Deposition along different random distributions could also have been investigated. Variation in density for more sticking rules, deposition onto different bases (as seen in Figure 19, for example), and deposition with a combination of sticking rules are all possible with the program, and could be both interesting and potentially more realistic.

REFERENCES

[1] Kiziridis, D. (2014). NetLogo Ballistic Deposition On-Lattice model. *Institute for Cross-Disciplinary Physics and Complex Systems, IFISC (CSIC-UIB)*

[2] F. Family, (1990*). Physica A,* 168, 561

[3] Penrose, M.D, (2008). 'Growth and roughness of the interface for ballistic deposition'. *Journal of Statistical Physics*, *131*(2), pp.247-268.

[4] Meakin, P., Ramanlal, P., Sander, L.M. and Ball, R.C., (1986). 'Ballistic deposition on surfaces.' *Physical Review A*, *34*(6), p.5091

[5] M.J. Vold, J. (1963). *Colloid Interface Sci*. 18, 684

[6] D.N. Sutherland, J. (1966). *Colloid Interface Sci.* 22, 300

[7] F. Family and T. Vicsek, J. (1985). *Phys. A* 18(2), L75

[8] Kardar,M.,Parisi,G.,Zhang,Y, (1986). 'Dynamic scaling of growing interfaces,' *Physics Review Letters* 56(9),889–892

[9] Robledo, A., Grabill, C.N., Kuebler, S.M., Dutta, A., Heinrich, H. and Bhattacharya, A., (2011). 'Morphologies from slippery ballistic deposition model: A bottom-up approach for nanofabrication.' *Physical Review E*, *83*(5), p.051604

[10] Miranda, R., Ramos, M. and Cadilhe, A., (2003). 'Finite-size scaling study of the ballistic deposition model in (1+ 1)-dimensions.' *Computational materials science*, *27*(1), pp.224-229

[11] Family, F.; Vicsek, T. (1985). "Scaling of the active zone in the Eden process on percolation networks and the ballistic deposition model". Journal of Physics A: Mathematical and General. 18 (2): L75–L81

[12] Schwettmann, A., (2003). 'Ballistic Deposition: Global Scaling and Local Time Series.'

[13] H. Fujiwara, K. Hara, M. Kamiya, 7: Hashimoto, K. Okamo- to, (1988). 'Comment on the tangent rule.' *Thin Solid Films,* 163. p.387-391

[14] Farnudi, B. and Vvedensky, D.D., (2011). 'Large-scale simulations of ballistic deposition: The approach to asymptotic scaling'. *Physical Review E*, *83*(2), p.020103

[15] El-Nashar, H.F., Wang, W. and Cerdeira, H.A., (1998). 'Growth morphology for a ballistic deposition model for multiple species.' *Physical Review E*, *58*(4), p.4461

[16] Forgerini, F.L. and Marchiori, R., (2014). 'A brief review of mathematical models of thin film growth and surfaces: A possible route to avoid defects in stents'. *Biomatter*, *4*(1), p.e28871

Word count: ~3350